On the Summation of Double Infinite Series Field Computations Inside Rectangular Cavities

Shahrokh Hashemi-Yeganeh, *Senior Member, IEEE*

Abstract—**An accurate and efficient computational technique for the full-wave analysis of passive microstrip lines inside rectangular cavities is described. The unique feature of the technique is the transformation of the double infinite series expansion of the method of moments solution into a few single summations of fast converging series using the residue theorem and the contour-integration method. The technique offers improved convergence especially when the field and source points coincide. Examples of the field computations inside the cavity are presented to verify the technique and its usefulness.**

I. Introduction

RECENTLY, considerable interest has been aroused in the theoretical modeling and field computations inside rectangular cavities or waveguides for such applications as packaging of microwave circuitry or antenna [1]–[7]. One of the common methods for the full-wave analysis of these models is the method of moment which utilizes the field Green's function solution pertinent to the rectangular enclosure of the cavity or the waveguide. The field expressions for these enclosures consist of nonseparable double infinite series of the Fourier sine and cosine modal expansions where the field boundary conditions are enforced. The standard technique to compute the series is the term-by-term summation of the modal summands and the examination of the result in progressive intervals for the convergence. Discrete fast Fourier transform has also been applied to the series where the periodicity of the sine and cosine functions are used to enhance the computational efficiency [5]. Nevertheless, this type of computation requires an exceedingly large number of modes for its convergence, and it is also dependent on the dimensions and type of basis and testing functions used in the method of moment solution. Furthermore, for the points that the source and field points coincide one may experience even slower convergence. In the following section an example of the field computations inside a probe-fed partially-filled cavity is examined. The residue theorem and the contour-integral method is used to improve the convergence of the computations and to determine the required number of modes. Theoretical and experimental results will be compared to verify the accuracy and efficiency of the method.

Manuscript received November 19, 1992; revised June 6, 1994.

The author was with the Department of Electrical Engineering, Arizona State University, Tempe, AZ 85287-7206, he is now withLJR Inc., El Secgundo, CA, 90245 USA.

IEEE Log Number 9408341.

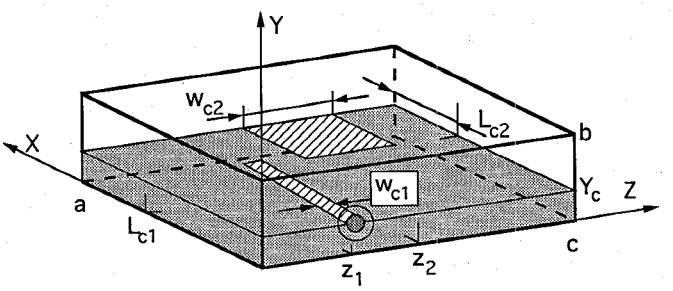

Fig. 1. Probe-fed partially filled rectangular cavity.

II. Formulation of the Probe-Fed Rectangular Cavity

Fig. 1 displays the probe-fed rectangular cavity. The probe is made of a thin narrow conducting strip which is separated from the bottom conductor by the dielectric substrate of thickness Y_c, and it is connected to the center conductor of a coaxial cable that feeds the cavity. The strip has rectangular periphery with the length and width pair of (L_{c1}, w_{c1}). A thin rectangular conducting patch of (L_{c2}, w_{c2}) has also been placed adjacent to the strip and electrically connected to the wall at $x = a$ for examining the proximity effect and the interaction between the patch and the strip. The strip and the patch are assumed to have zero thickness. The walls of the cavity, the strip, and the patch are made of perfect conductors while the dielectric can take on small loss.

The coupling of the energy and its subsequent storage in the cavity can be formulated by the summation of the modal electric and magnetic fields inside the cavity while satisfying the boundary conditions on the strip and patch conductors. This condition can be represented by the following set of coupled integral equations in terms of the sought-for surface currents on the strip and the patch:

$$\vec{E}_{\tan}(P_1, P_1') + \vec{E}_{\tan}(P_1, P_2') = -f(x, Y_c, z)\vec{a}_x \quad \text{(1a)}$$

$$\vec{E}_{\tan}(P_2, P_1') + \vec{E}_{\tan}(P_2, P_2') = 0 \quad \text{(1b)}$$

where

$$f(x, Y_x, z) = \begin{cases} \delta(x) & z_1 \le z \le z_1 + w_{c1}, \quad y = Y_c \\ 0 & \text{otherwise} \end{cases}. \quad (2)$$

$\vec{E}_{\tan}$ is the internal tangential electric field at $y = Y_c^+$ inside the cavity. The pair $(P_i(x, Y_c, z), P_i'(x', Y_c, z'))$ are, respectively, the field and the source points on the strip $(i = 1)$

or the patch ($i = 2$) conductors. $f(x, Y_c, z)$ is a delta function generator for modeling the coaxial line feed at $x = 0$. It is assumed that the strip is so narrow ($w_{c1} \ll L_{c1}$) that only x-directed current exists along it, whereas the patch is wide enough to include both x- and z-directed currents on its surface.

The method of moments with Galerkin technique is applied to the equations in (1) to determine approximately the surface current distributions. The basis functions for these currents consist of separable piecewise sinusoidal and pulse functions. Fig. 2 displays the arrangement of these functions for the strip and the patch conductor currents. To approximate the input current into the strip at $x = 0$ and the current passing through the patch corner junction at $x = a$ half piecewise sinusoidals are added to the corresponding basis functions.

Green's functions for the integral equations in (1) consist of the summations of the infinite numbers of TE^y and TM^y modal fields that are matched at $y = Y_c^+$ and satisfy the boundary conditions on the walls [2]. They are given by (3), (4), shown at the bottom of the page, and (5)–(7).

$$\begin{bmatrix} E_x(x, Y_c, z) \\ E_z(x, Y_c, z) \end{bmatrix} = \frac{4j}{\omega\varepsilon_1 ac} \sum_{m=0}^{\infty}\sum_{n=0}^{\infty} \frac{\bar{\varepsilon}_m \bar{\varepsilon}_n}{\gamma_{mn1}} \begin{bmatrix} \Phi_{mn}(x,y)(\vec{a}_x f_{1ma} + \vec{a}_z f_2) \\ \Psi_{mn}(x,y)(\vec{a}_x f_2 + \vec{a}_z f_{1nc}, \end{bmatrix} \cdot \int_{\text{conductor}} [\vec{a}_x K_x(x', Y_c, z')\Phi_{mn}(x', y') + \vec{a}_z K_z(x', Y_c', z')\Psi_{mn}(x', y')]dx'dz' \tag{3}$$

$$f_2 = \frac{(\frac{m\pi}{a})(\frac{n\pi}{c})[\coth(\gamma_{mn1}(b - Y_c)) + \frac{\gamma_{mn1}}{\gamma_{mn2}}\coth(\gamma_{mn2}Y_c)]}{g_{mn}} \tag{5}$$

$$g_{mn} = \left[\coth(\gamma_{mn1}(b - Y_c)) + \frac{\gamma_{mn2}}{\gamma_{mn1}}\coth(\gamma_{mn2}Y_c)\right] \times \left[\coth(\gamma_{mn1}(b - Y_c)) + \frac{\varepsilon_2}{\varepsilon_1}\frac{\gamma_{mn1}}{\gamma_{mn2}}\coth(\gamma_{mn2}Y_c)\right] \tag{6}$$

$$\begin{bmatrix} \Phi_{mn}(x,z) \\ \Psi_{mn}(x,z) \end{bmatrix} = \cos\begin{bmatrix} \frac{m\pi x}{a} \\ \frac{n\pi z}{c} \end{bmatrix} \sin\begin{bmatrix} \frac{n\pi z}{c} \\ \frac{m\pi x}{a} \end{bmatrix} \tag{7}$$

$\gamma_{mni} = \sqrt{(\frac{m\pi}{a})^2 + (\frac{n\pi}{c})^2 - k_i^2}$ and $\bar{\varepsilon}_i = \begin{cases} 1/2 & i = 0 \\ 1 & i \neq 0 \end{cases} \cdot k_j = \omega\sqrt{\mu_j \varepsilon_j}$, $j = (1, 2)$, are the propagation constants of the two different media inside the cavity with the constitutive parameters of ε_j and μ_j. K_x and K_z are the surface current components on the strip or the patch. In this analysis, $j = 1$ and $j = 2$ refer to the air-filled and the dielectric-filled regions of the cavity, respectively. Application of the method of moments with the aforementioned basis and testing functions transforms the integral equations in (1) into a set of simultaneous linear equations in the matrix form $[Z_{P,P'}]\ [K_{P'}] = [V_P]$. The elements of $[Z_{P,P'}]$ consist of double infinite summations of the interacting fields on the strip and the patch. Four of these elements are

$$\begin{aligned} &Z_{Ex1,Kx2}(I_{x1}, Y_c, J_{x1}; I'_{x2}, Y_c, J'_{x2}) \\ &= \frac{16j}{\omega\varepsilon_1 ac}\left[\frac{4k_0}{\sin(k_0\Delta x_1)}\right]\left[\frac{4k_0}{\sin(k_0\Delta x_2)}\right]\sum_{m=0}^{\infty}\sum_{n=1}^{\infty}\frac{\bar{\varepsilon}_m}{\gamma_{mn1}} \\ &\cdot F_{1ma}\frac{\sin(\frac{n\pi}{c}\frac{\Delta z_1}{2})}{(\frac{n\pi}{c})}\frac{\sin(\frac{n\pi}{c}\frac{\Delta z_2}{2})}{(\frac{n\pi}{c})} \\ &\times \frac{\Lambda_m(a, \Delta x_1)\Lambda_m(a, \Delta x_2)}{[(\frac{m\pi}{a})^2 - k_0^2]}\bar{\varepsilon}_{I_{x1}} \\ &\times \Phi_{mn}\left(I_{x1}\Delta x_1, z_1 + \left(J_{x1} - \frac{1}{2}\right)\Delta z_1\right) \\ &\cdot \sum_{J'_{x2}=1}^{NZC2}\sum_{I'_{x2}=1}^{NXC2} Kx_{I'_{x2},J'_{x2}}\bar{\varepsilon}_{NXC2-I'_{x2}} \\ &\times \Phi_{mn}\left(x_2 + I'_{x2}\Delta x_2, z_2 + \left(J'_{x2} - \frac{1}{2}\right)\Delta z_2\right) \\ &= Z_{Ex2,Kx1}(I'_{x2}, Y_c, J'_{x2}; I_{x1}, Y_c, J_{x1}) \end{aligned} \tag{8}$$

$$\begin{aligned} &Z_{Ex1,Kz2}(I_{x1}, Y_c, J_{x1}; I'_{z2}, Y_c, J'_{z2}) \\ &= \frac{16j}{\omega\varepsilon_1 ac}\left[\frac{4k_0}{\sin(k_0\Delta x_1)}\right]\left[\frac{4k_0}{\sin(k_0\Delta z_2)}\right]\sum_{m=1}^{\infty}\sum_{n=1}^{\infty}\frac{F_2}{\gamma_{mn1}} \\ &\cdot \sin\left(\frac{m\pi}{a}\frac{\Delta x_2}{2}\right)\sin\left(\frac{n\pi}{c}\frac{\Delta z_1}{2}\right) \\ &\times \frac{\Lambda_m(a, \Delta x_1)\Lambda_n(c, \Delta z_2)\bar{\varepsilon}_{I_{x1}}}{[(\frac{m\pi}{a})^2 - k_0^2]\,[(\frac{n\pi}{c})^2 - k_0^2]} \\ &\times \Phi_{mn}\left(I_{x1}\Delta x_1, z_1 + \left(J_{x1} - \frac{1}{2}\right)\Delta z_1\right) \\ &\cdot \sum_{J'_{z2}=1}^{NZC2-1}\sum_{I'_{z2}=1}^{NXC2} Kz_{I'_{z2}J'_{z2}}\Psi_{mn} \\ &\times \left(x_2 + \left(I'_{z2} - \frac{1}{2}\right)\Delta x_2, z_2 + J'_{z2}\Delta z_2\right) \\ &= Z_{Ez2,Kx1}(I'_{z2}, Y_c, J'_{z2}; I_{x1}, Y_c, J_{x1}) \end{aligned} \tag{9}$$

where

$$F_{1id} = \frac{f_{1id}}{[(\frac{i\pi}{d})^2 - k_0^2]},\quad F_2 = \frac{f_2}{(\frac{m\pi}{a})(\frac{n\pi}{c})},\quad \text{and}$$

$$\Lambda_p(d, \Delta) = \sin\left[\left(\frac{p\pi}{d} + k_0\right)\frac{\Delta}{2}\right]\cdot\sin\left[\left(\frac{p\pi}{d} - k_0\right)\frac{\Delta}{2}\right].$$

Also $I_{x1} = 0, \cdots, NXC1 - 1, J_{x1} = 1, \cdots, NZC1, \Delta z_1 \times NZC1 = w_{c1}, \Delta x_1 \times NXC1 = L_{c1}, \Delta z_2 \times NZC2 = w_{c2}$, and $\Delta x_2 \times NXC2 = L_{c2}$. The remaining elements

$$f_{1id} = \frac{[(\frac{i\pi}{d})^2 - k_1^2]\coth(\gamma_{mn1}(b - Y_c)) + [(\frac{i\pi}{d})^2 - k_2^2]\frac{\gamma_{mn1}}{\gamma_{mn2}}\coth(\gamma_{mn2}Y_c)}{g_{mn}} \tag{4}$$

can be obtained by the minor alterations of (8) and (9). Finally, V_P is the excitation model by the coaxial aperture at $x = 0$ (see (2)), and it is given by $V_P = \left\{ \begin{matrix} -\Delta z_1 & I_{x1} = 0, J_{x1} = 1, \cdots, NZC1 \\ 0 & \text{otherwise} \end{matrix} \right\}$. The solution of (1) can be obtained by the inversion to the form $[K_{P'}] = [Z_{P,P'}]^{-1}[V_P]$.

III. Computational Technique

The double infinite series in $[Z_{P,P'}]$ can be computed efficiently using the residue theorem and the contour integral method. For instance, consider the series in (8). It can be accurately approximated by the following double summations:

$$
\begin{aligned}
&Z_{Ex1,Kx2}(I_{x1}, Y_c, J_{x1}; I'_{x2}, Y_c, J'_{x2}) \\
&= \frac{16j}{\omega\varepsilon_1 ac}\left[\frac{4k_0}{\sin(k_0\Delta x_1)}\right]\left[\frac{4k_0}{\sin(k_0\Delta x_2)}\right] \\
&\cdot \left\{ \sum_{m=0}^{M_1}\sum_{n=1}^{N_1} \frac{\bar{\varepsilon}_m}{\gamma_{mn\,1}} F_{1\,ma} \frac{\sin\left(\frac{n\pi}{c}\frac{\Delta z_1}{2}\right)}{\left(\frac{n\pi}{c}\right)} \frac{\sin\left(\frac{n\pi}{c}\frac{\Delta z_2}{2}\right)}{\left(\frac{n\pi}{c}\right)} \right. \\
&\times \frac{\Lambda_m(a,\Delta x_1)\Lambda_m(a,\Delta x_2)}{\left[\left(\frac{m\pi}{a}\right)^2 - k_0^2\right]} \\
&\cdot \bar{\varepsilon}_{I_{x1}} \Phi_{mn}\left(I_{x1}\Delta x_1, z_1 + \left(J_{x1} - \frac{1}{2}\right)\Delta z_1\right) \\
&\cdot \sum_{J'_{x2}=1}^{NZC2}\sum_{I'_{x2}=1}^{NXC2} Kx_{I'_{x2}J'_{x2}} \bar{\varepsilon}_{NXC2-I'_{x2}} \\
&\times \Phi_{mn}\left(x_2 + I'_{x2}\Delta x_2, z_2 + \left(J'_{x2} - \frac{1}{2}\right)\Delta z_2\right) \\
&+ \sum_{m=M_1+1}^{M_2}\sum_{n=1}^{N_2} \frac{1}{\gamma_{mn\,1}}\left[F_{1ma} - \frac{P_m}{2(1+\varepsilon_2/\varepsilon_1)}\right] \\
&\times \frac{\sin\left(\frac{n\pi}{c}\frac{\Delta z_1}{2}\right)}{\left(\frac{n\pi}{c}\right)} \frac{\sin\left(\frac{n\pi}{c}\frac{\Delta z_2}{2}\right)}{\left(\frac{n\pi}{c}\right)} \frac{\Lambda_m(a,\Delta x_1)\Lambda_m(a,\Delta x_2)}{\left[\left(\frac{m\pi}{a}\right)^2 - k_0^2\right]} \\
&\cdot \bar{\varepsilon}_{I_{x1}} \Phi_{mn}\left(I_{x1}\Delta x_1, z_1 + \left(J_{x1} - \frac{1}{2}\right)\Delta z_1\right) \\
&\cdot \sum_{J'_{x2}=1}^{NZC2}\sum_{I'_{x2}=1}^{NXC2} Kx_{I'_{x2}J'_{x2}} \bar{\varepsilon}_{NXC2-I'_{x2}} \\
&\times \Phi_{mn}\left(x_2 + I'_{x2}\Delta x_2, z_2 + \left(J'_{x2} - \frac{1}{2}\right)\Delta z_2\right) \\
&+ \frac{1}{16(\frac{\pi}{c})^3(1+\varepsilon_2/\varepsilon_1)} \\
&\times \sum_{m=M_1+1}^{\infty} P_m \frac{\Lambda_m(a,\Delta x_1)\Lambda_m(a,\Delta x_2)}{\left[\left(\frac{m\pi}{a}\right)^2 - k_0^2\right]} \\
&\cdot \bar{\varepsilon}_{I_{x1}} \cos\left(\frac{m\pi}{a}(I_{x1}\Delta x_1)\right) \\
&\times \sum_{J'_{x2=1}}^{NZC2}\sum_{I'_{x2}=1}^{NXC2} Kx_{I'_{x2}J'_{x2}} \bar{\varepsilon}_{NXC2-I'_{x2}} \\
&\left. \times \cos\left(\frac{m\pi}{a}(x_2 + I_{x2}\Delta x_2)\right) \cdot \sum_{r=1}^{8} w_r G_n(|Z_r|, A_m) \right\} \qquad (10)
\end{aligned}
$$

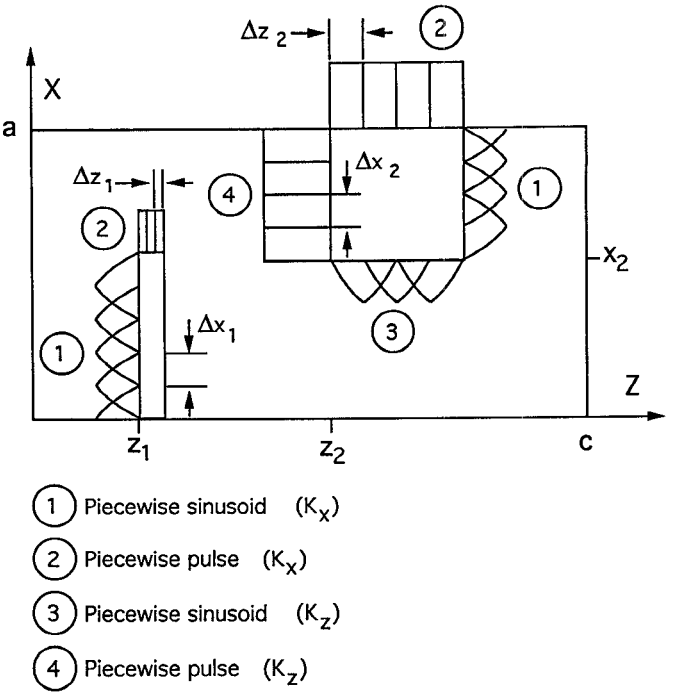

Fig. 2. Arrangement of the basis and testing functions on the conductor surfaces.

where

$$P_m = \frac{(\frac{m\pi}{a})^2 - k_1^2}{(\frac{m\pi}{a})^2 - k_0^2} + \frac{(\frac{m\pi}{a})^2 - k_2^2}{(\frac{m\pi}{a})^2 - k_0^2}, \qquad (11)$$

$$G_n(z, A) = \sum_{n=1}^{\infty} \frac{\cos(nz)}{n^2\sqrt{n^2 + A^2}}, \qquad (12)$$

$$Z_{\frac{1}{2}} = \frac{\pi}{c}(z_1 + J_{x1}\Delta z_1 \pm z_2 \pm J'_{x2}\Delta z_2), \qquad (13a)$$

$$Z_{\frac{3}{4}} = \frac{\pi}{c}(z_1 + (J_{x1} - 1)\Delta z_1 \pm z_2 \pm (J'_{x2} - 1)\Delta z_2), \qquad (13b)$$

$$Z_{\frac{5}{6}} = \frac{\pi}{c}(z_1 + J_{x1}\Delta z_1 \pm z_2 \pm (J'_{x2} - 1)\Delta z_2), \qquad (13c)$$

$$Z_{\frac{7}{8}} = \frac{\pi}{c}(z_1 + (J_{x1} - 1)\Delta z_1 \pm z_2 \pm J'_{x2}\Delta z_2), \qquad (13d)$$

$$A_m = \frac{\sqrt{(\frac{m\pi}{a})^2 - k_1^2}}{\frac{\pi}{c}}, \qquad (14)$$

and $w_r = \left\{ \begin{matrix} 1 & 1 \le r \le 4 \\ -1 & 5 \le r \le 8 \end{matrix} \right\}$. The integers N_1, M_1, N_2, and M_2 are set by the following conditions: $1 - M_1 \ge 1 + (a/\pi)\sqrt{|k_2|^2 - (\pi/c)^2}$ and $N_1 \ge 1000$. $2 - M_2 = \text{Max}(M_{21}, M_{22})$ and $N_2 = \text{Max}(N_{21}, N_{22})$ where $M_{21} \ge h(a, c, s_1)$, $M_{22} \ge h(a, c, s_2)$, $N_{21} \ge h(c, a, s_1)$, $N_{22} \ge h(c, a, s_2)$, $h(d_1, d_2, s) = (d_1/\pi)\sqrt{|k_2|^2 - (\pi/d_2)^2 + s^2}$, $s_1 = -\ln(\delta_1)/Y_{\min}$, $s_2 = (1-\delta_2)\sqrt{(|k_2|^2 - k_1^2)/(2\delta_2 - \delta_2^2)}$, $Y_{\min} = \text{Min}(Y_c, b - Y_c)$, $\delta_1 = 10^{-6}$, and $\delta_2 = 10^{-3}$. While these conditions set the upper limit on the increasing values of m and n for $|\coth(\ldots)| \to 1, |\gamma_{mn2}/\gamma_{mn1}| \to 1$, and $|P_m| \to 2$, the added decay of the summands by $\sim 1/m^3$ and $\sim 1/n^3$ in (10) greatly enhances the rapid convergence of the series. Consequently, the conditions set above for δ_1 and δ_2 are sufficient for these computations. Next, fast converging

series to substitute for the latter double summation in (10) are introduced.

The n-series in the last double summation of (10) can be transformed into an exponentially converging series using residue theorem and the theory of contour integration in the complex plane [8], [9]. To begin the transformation, consider the following contour integral

$$\oint_{C_n} \frac{1}{z^2\sqrt{z^2+A^2}} \frac{e^{j\alpha z}}{(e^{j2\pi z}-1)}\, dz \tag{15}$$

where the contour C_n is depicted in Fig. 3. It consists of the large circular path of radius $R = n + (1/2)$, the paths parallel to the branch lines along $z \leq -jA$ and $z \geq +jA$, and the small circles of radius $r \rightarrow 0$ around the branch points at $z = \pm jA$. The contour is chosen large enough so it encompasses all the poles of the integrand, while it excludes the branch points and the branch lines. The factor $(e^{j2\pi z} - 1)$ creates the poles at the integer values $\pm n$. As the $n \rightarrow \infty$, the closed line integral over C_n vanishes. Using the Cauchy's integral formula and the residue theorem [8], [9], the integral in (15) can be transformed into

$$\begin{aligned} G_n(\alpha, A) &= \sum_{n=1}^{n=\infty} \frac{\cos(n\alpha)}{n^2\sqrt{n^2+A^2}} \\ &= \frac{1}{4A^3} + \frac{(\pi-\alpha)^2}{4A} - \frac{\pi^2}{12A} \\ &\quad - \int_{Z=A}^{z=\infty} \frac{1}{z^2\sqrt{z^2-A^2}} \frac{\cosh[z(\pi-\alpha)]}{\sinh(z\pi)}\, dz \end{aligned} \tag{16}$$

for $0 < \alpha < 2\pi$. The ratio of the hyperbolic functions in (16) can be easily expanded by infinite series of fast-decaying exponential functions. Hence, (16) can be written as

$$\begin{aligned} &G_n(\alpha, A) \\ &\quad = \frac{1}{4A^3} + \frac{(\pi-\alpha)^2}{4A} - \frac{\pi^2}{12A} \\ &\qquad - \frac{1}{A^2} \sum_{q=0}^{\infty} \int_{t=1}^{t=\infty} \frac{(e^{-tA(2q\pi+\alpha)} + e^{-tA(2(q+1)\pi-\alpha)})}{t^2\sqrt{t^2-1}}\, dt. \end{aligned} \tag{17}$$

An integral in (17) can be replaced by two consecutive integrations of the modified Bessel function of zeroth order, K_0 [10],

$$\begin{aligned} Ki_2(x) &= \int_{z=x}^{z=\infty} Ki_1(z)dz = \int_{z=x}^{z=\infty} \left(\int_{y=z}^{y=\infty} K_0(y)dy \right) dz \\ &= \int_{t=1}^{t=\infty} \frac{e^{-xt}}{t^2\sqrt{t^2-1}}\, dt \end{aligned} \tag{18}$$

where $Ki_1(x)$ and $Ki_2(x)$ can be obtained from (11.1.9), (11.1.18), and (11.2.8) in [10]. Therefore, $G_n(\alpha, A)$ becomes equal to

$$\begin{aligned} &G_n(\alpha, A) \\ &\quad = \frac{1}{4A^3} + \frac{(\pi-\alpha)^2}{4A} - \frac{\pi^2}{12A} \\ &\qquad - \frac{1}{A^2} \sum_{q=0}^{\infty} (Ki_2[A(2q\pi+\alpha)] + Ki_2[A(2(q+1)\pi-\alpha)]). \end{aligned} \tag{19}$$

$Ki_2(x)$ function has asymptotic exponential decay for the arguments $x \geq 7$. If (19) is utilized in (10), the last double summation can be converted to eight dominant single summations plus eight rapidly converging double summations with Ki_2 functions in the summands and increasing A_m in their arguments. The fast asymptotic decaying behavior of Ki_2 function allows one to evaluate the last summation with any desired accuracy. To do this, the summation on $\underline{m}$ is divided into two parts. In the first part, the summation is performed from $m = M_1 + 1$ to M_3 where the Ki_2's are included. In the second part, the summation from $m = M_3 + 1$ to $m = \infty$ is performed where Ki_2's are set to zero. This is justified since they contribute exponentially small terms to the summation. The integer M_3 can be determined by imposing an upper bound on the sums of Ki_2 terms in the second part, with respect to the first part. The upper bound for the summation $\sum_{m=M_3+1}^{\infty} e^{-A_m Z_{\min}}$ and hence M_3 integer, where $Z_{\min} = (|Z_i|, i = 1, \cdots, 8)$, can be obtained by the following condition

$$\frac{\left\lfloor \frac{e^{c\,k_1 Z_{\min}/\pi}}{1-e^{-cZ_{\min}/2}} \right\rfloor e^{-(M_3+1)cZ_{\min}/a}}{\sum_{m=M_1+1}^{M_3} e^{-A_m Z_{\min}}} < \delta_0 \tag{20}$$

where $\delta_0 \ll 1$ is the condition for reducing the error due to the Ki_2's elimination. It should be noted that the condition in (20) does not include any additional converging term such as $\sim 1/m^3$ which is multiplied by the Ki_2 summations and further improves the total convergence. Finally, the limiting value of the integers q's are set by an upper bound on the arguments of the exponential functions. If one implements the above procedure, the last double summation in (10) can be accurately approximated by

$$\begin{aligned} &+ \frac{1}{16(\frac{\pi}{c})^3(1+\varepsilon_2/\varepsilon_1)} \sum_{m=M_1+1}^{M_3} P_m \frac{\Lambda_m(a,\Delta x_1)\Lambda_m(a,\Delta x_2)}{[(\frac{m\pi}{a})^2 - k_0^2]} \\ &\quad \cdot \bar{\varepsilon}_{I_{x1}} \cos\left(\frac{m\pi}{a}(I_{x1}\Delta x_1)\right) \sum_{J'_{x2}=1}^{NZC2} \sum_{I'_{x2}=1}^{NXC2} Kx_{I'_{x2}J'_{x2}} \bar{\varepsilon}_{NXC2-I'_{x2}} \\ &\quad \times \cos\left[\frac{m\pi}{a}(x_2 + I_{x2}\Delta x_2)\right] \cdot \sum_{r=1}^{8} w_r G_n(|Z_r|, A_m) \\ &+ \frac{1}{16(\frac{\pi}{c})^3(1+\varepsilon_2/\varepsilon_1)} \sum_{m=M_3+1}^{\infty} P_m \frac{\Lambda_m(a,\Delta x_1)\Lambda_m(a,\Delta x_2)}{[(\frac{m\pi}{a})^2 - k_0^2]} \\ &\quad \cdot \bar{\varepsilon}_{I_{x1}} \cos\left(\frac{m\pi}{a}(I_{x1}\Delta x_1)\right) \sum_{J'_{x2}=1}^{NZC2} \sum_{I'_{x2}=1}^{NXC2} Kx_{I'_{x2}J'_{x2}} \bar{\varepsilon}_{NXC2-I'_{x2}} \\ &\quad \times \cos\left[\frac{m\pi}{a}(x_2 + I_{x2}\Delta x_2)\right] \\ &\quad \cdot \sum_{r=1}^{8} w_r \left[\frac{1}{4A_m^3} + \frac{(\pi - |Z_r|)^2}{4A_m} - \frac{\pi^2}{12A_m} \right] \end{aligned} \tag{21}$$

where the last series in (21) has been reduced into a single summation in $\underline{m}$. Since in this approximation both series converge as $\sim 1/m^3$, it is possible to choose a less severe condition on the final $\underline{m}$ for the two series while using the above accelerated series for the n-series.

The remaining double summations in $[Z_{P,P'}]$ can also be expanded to similar fast converging series as discussed above.

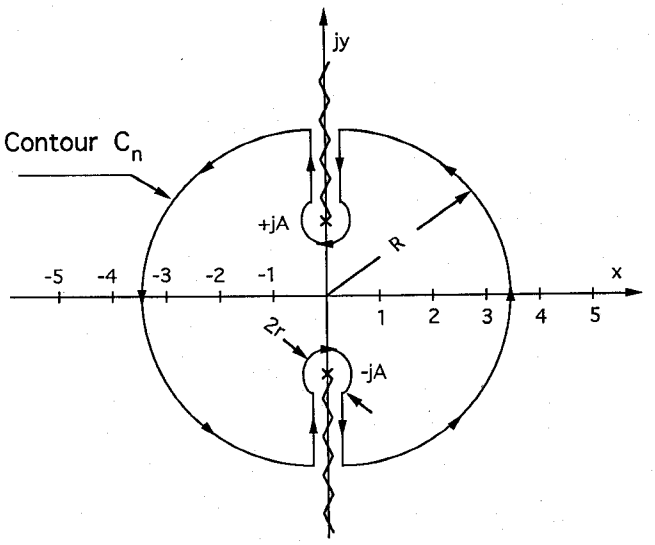

Fig. 3. Contour C_n with the branch lines and the branch points.

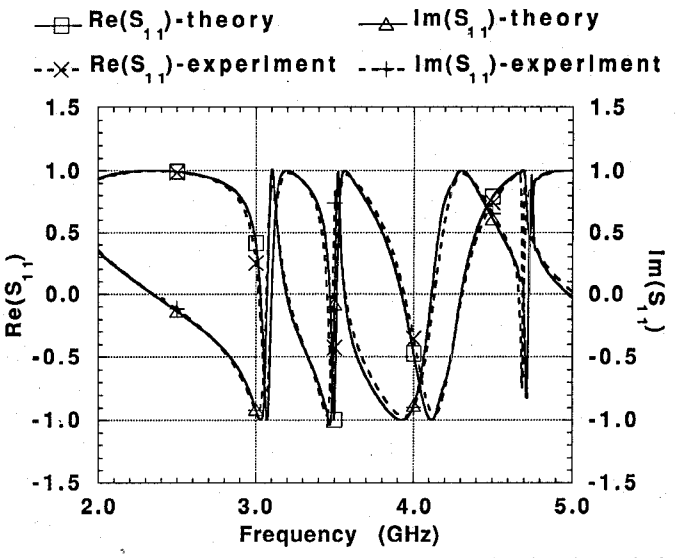

Fig. 4. Reflection coefficient versus frequency of the closed cavity excited by the open ended narrow strip with the patch: $a = 4.953$ cm, $b = 2.179$ cm, $c = 6.985$ cm, $z_1 = 2.4725$ cm, $L_{c1} = 4.22$ cm, $w_{c1} = 0.135$ cm, $x_2 = 3.467$ cm, $z_2 = 2.765$ cm, $L_{c2} = 1.486$ cm, $w_{c2} = 0.445$ cm, $Y_c = 0.635$ cm, and $\epsilon_{r_2} = 2.2$

IV. Numerical and Experimental Results

In order to verify the theoretical model and the computational technique described, an experimental model similar to Fig. 1 was built and tested. In the absence of any slot or sizable opening, the input impedance at $x = 0$ becomes purely reactive if the ohmic losses due to the conducting walls, the strip, the patch, and the dielectric in the cavity are ignored. Fig. 4 displays the computed and measured values of the reflection coefficients versus frequency of the model. The dimensions of the cavity, the strip, and the patch were $a = 4.953$ cm, $b = 2.179$ cm, $c = 6.985$ cm, $L_{c1} = 4.22$ cm ($NXC1 = 20$), $w_{c1} = 0.135$ cm ($NZC1 = 3$), $L_{c2} = 1.486$ cm ($NXC2 = 20$), $w_{c2} = 0.445$ cm ($NZC2 = 6$), $Y_c = 0.635$ cm, $z_1 = 2.4725$ cm, $x_2 = 3.467$ cm, and $z_2 = 2.765$ cm. The relative permittivities of the two media were $\varepsilon_{r1} = 1$ and $\varepsilon_{r2} = 2.2$ (RT/duroid 5880[1]). Computed values for $k_0 = 5$ [2] are represented by the solid line while the measured data is represented by the dashed lines. $M_3 = 500$ was the total number of $\underline{m}$ used in the first series of (21) while the second series was excluded from the computation. The CPU time on the IBM RISC 6000 required for a single frequency computation was less than four minutes. The differences between the theory and the measurement are seen to be small. The optimum number of cells used in this simulation was determined by a few trials for the convergence of the above test. In the case of patch current a more stringent condition of quasi square cells for the basis and testing functions was imposed to allow equal weight consideration for the x- and z-directed currents.

Next, a pair of L-shaped narrow strips unsymmetrically positioned around $x = a/2$ and $z = c/2$ center lines was simulated. Fig. 5 shows the arrangement of the pair inside the cavity. The dimensions were $a = 1.44$ cm, $b = 1.5$ cm, $c = 3.0$ cm, $Y_c = 0.2$ cm, and $w = 0.135$ cm. Fig. 6 shows the associated S-parameters in the frequency range of 2.0 GHz

[1]The laminate was provided by Rogers Corporation 100 S. Roosevelt Ave., Chandler, AZ 85226.

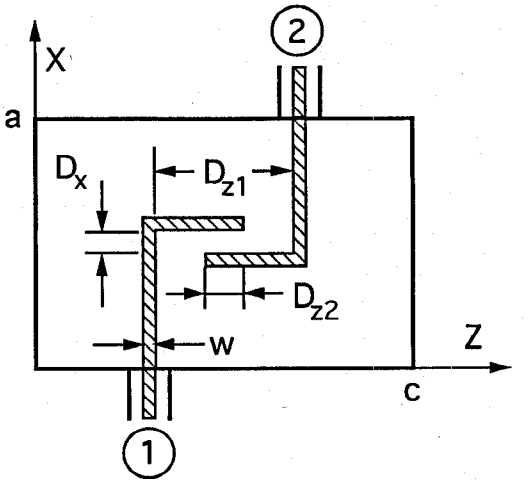

Fig. 5. Arrangement of the pair of the L-shaped strips inside the cavity.

$\leq \nu \leq 5.0$ GHz for $D_x = 0.09$ cm, $D_{z1} = (1.26, 1.08)$ cm, $D_{z2} = (0.36, 0.54)$ cm, and $\varepsilon_{r2} = 2.2 \times (1 - jL(\nu))$ where the loss tangent $L(\nu) = 5.0005 \times 10^{-5}\ (\nu - 0.001) + 0.0004$ was assumed. The number of basis and testing functions used in the simulation were 3 and 40 along the width and the length of each strip, respectively. The selection of these numbers provided square shape cells as well as proper overlapping of the cross-polarized currents at the corners of the L-shaped strips. As it can be seen the coupling between the strips is inversely proportional to D_{z1} and directly proportional to D_{z2}.

Computation of $[Z_{P,P'}]$ based on simple repetitive summation of the summands required large numbers of the $\underline{m}$ and $\underline{n}$ integer variables. For the total number of modes $m = 500$, and $n = 500(c/a)$, the CPU time needed for a single frequency computation was more than four times of the above accelerated cases. This shows a considerable time saving and accuracy for the computational technique.

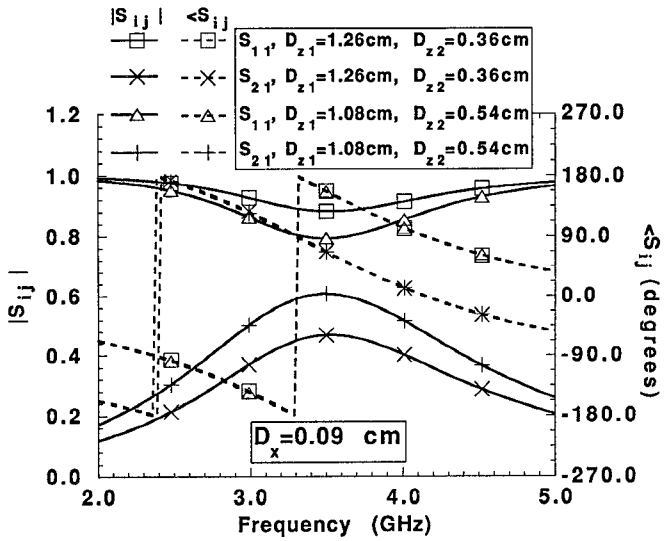

Fig. 6. Scattering parameters of the pair of the L-shaped strips for $D_x = 0.09$ cm ($a = 1.44$ cm, $b = 1.5$ cm, $c = 3.0$ cm, $w_c = 0.135$ cm, $Y_c = 0.2$ cm, $\epsilon_{r2} = 2.2 \times (1L(v) = 5.0005 \times 10^5(v - 0.001) + 0.0004)$.

V. Conclusion

In this study the full-wave analysis of the probe-fed partially-filled rectangular cavity was undertaken. The method of moment solution of the unknown strip current inside the cavity was developed, and it was accurately evaluated by the computational technique. Two important outcomes of this study were the noticeable time-saving and the theoretical means of determining the upper bound on the number of modes required for the convergence. This can be helpful in the repeated simulations of similar problems with larger cavity dimensions or the unknown currents. Finally, for the problems where the cavity is filled partially with multilayered dielectrics, the modified forms of the F_{1id} and F_2 expressions and their asymptotic forms can be utilized to implement the technique as well.

Acknowledgment

The author would like to thank Mr. C. R. Birtcher at the Arizona State University for the fabrication of the test unit and for help with measurements.

References

[1] J. C. Rautio and R. F. Harrington, "An electromagnetic time-harmonic analysis of shielded microstrip circuits," *IEEE Trans. Microwave Theory Tech.*, vol. MTT-35, no. 8, pp. 726–730, Aug. 1987.

[2] L. P. Dunleavy and P. B. Katehi, "A generalized method for analyzing shielded thin microstrip discontinuities," *IEEE Trans. Microwave Theory Tech.*, vol. 36, no. 12, pp. 1758–1766, Dec. 1988.

[3] ——, "Shielding effects in microstrip discontinuities," *IEEE Trans. Microwave Theory Tech.*, vol. 36, no. 12, pp. 1767–1774, Dec. 1988.

[4] A. Hadidi and M. Hamid, "Aperture field and circuit parameters of cavity-backed slot radiator," *IEEE Proc.*, vol. 136, Pt. H, pp 139–146, Apr. 1989.

[5] A. Hill and V. K. Tripathi, "An efficient algorithm for the three-dimensional analysis of passive microstrip components and discontinuities for microwave and millimeter-wave integrated circuits," *IEEE Trans. Microwave Theory Tech.*, vol. 39, no. 1, pp. 83–91, Jan. 1991.

[6] N. L. VandenBerg, P. B. Katehi, J. A. Lick, and G. T. Mooney, "Characterization of strip-fed cavity-backed slots," *IEEE Trans. Microwave Theory Tech.*, vol 40, no. 4, pp. 405–413, Apr. 1992.

[7] S. Hashemi-Yeganeh and C. Birtcher, "Theoretical and experimental studies of cavity-backed slot antenna excited by a narrow strip," *IEEE Trans. Antennas Propagat*, vol. 41, no. 2, pp. 236–241, Feb. 1993.

[8] R. E. Collin, *Field Theory of Guided Waves*. New York: McGraw-Hill, 1960, pp. 577–585.

[9] M. R. Spiegel, *Complex Variable*, Schaum's Outline Series in Mathematics. New York: McGraw-Hill, 1964, ch. 7.

[10] M. Abramowitz and I. A. Stegen, *Handbook of Mathematical Functions*. New York: Dover, 1970, pp. 480–483.

Shahrokh Hashemi-Yeganeh (S'88–M'88–SM'93), for a photograph and biography, see p. 1068 of the June 1994 issue of this TRANSACTIONS.